Chemical Engineering Journal 150 (2009) 25–39

Contents lists available at ScienceDirect

Chemical Engineering Journal

journal homepage: www.elsevier.com/locate/cej

Removal of chromium(VI) from wastewater by activated carbon developed from *Tamarind wood* activated with zinc chloride

Jyotikusum Acharya[a], J.N. Sahu[b], B.K. Sahoo[b], C.R. Mohanty[c], B.C. Meikap[b,*]

[a] *School of Energy and Environment Management, Rajiv Gandhi Proudyogiki Vishwavidyalaya, Gandhinagar, Bhopal, Madhya Pradesh, India*
[b] *Department of Chemical Engineering, Indian Institute of Technology (IIT), Kharagpur, P.O. Kharagpur Technology, West Bengal 721302, India*
[c] *State Pollution Control Board, Orissa (Department of Forest & Environment, Govt. of Orissa) Paribesh Bhawan, Bhubaneswar 751012, India*

ARTICLE INFO

Article history:
Received 6 October 2008
Received in revised form
18 November 2008
Accepted 21 November 2008

Keywords:
Chromium removal
Activated carbon
Chemical activation
Zinc chloride
Adsorption
Wastewater treatment

ABSTRACT

In this work, the adsorption of chromium(VI) was studied on activated carbon prepared from *Tamarind wood* with zinc chloride activation. Adsorption studies were conducted in the range of 10–50 mg/l initial chromium(VI) concentration and at temperature in the range of 10–50 °C. The experimental data were analyzed by the Freundlich isotherm and the Langmuir isotherm. Equilibrium data fitted well with the Langmuir model and Freundlich model with maximum adsorption capacity of 28.019 mg/g. The rates of adsorption were found to confirm to pseudo-second-order kinetics with good correlation and the overall rate of chromium(VI) uptake was found to be controlled by pore diffusion, film diffusion and particle diffusion, throughout the entire adsorption period. Boyd plot confirmed that external mass transfer was the rate-limiting step in the adsorption process. Different thermodynamic parameters, viz., ΔH°, ΔS° and ΔG° have also been evaluated and it has been found that the adsorption was feasible, spontaneous and endothermic in nature. The results indicate that the *Tamarind wood* activated could be used to effectively adsorb chromium(VI) from aqueous solutions.

1. Introduction

Chromium compounds are among the most dangerous inorganic water pollutants. Chromium is considered to be one of the priority pollutants, chromium is soluble in water and hence mobile and it possesses a great threat to surface and ground water quality, which is a threat to human health. The rapid development and proliferation of process industries have made wastewater treatment a major concern in industrial areas. The presence of metal ions in natural (mainly by volcanic activity and weathering of rocks) [1] or industrial wastewater and their potential impact has been a subject of research in environmental science for a long time. Chromium compounds mainly occur in the environment as trivalent, Cr(III), and hexavalent, chromium(VI), chromium. Trivalent chromium is an essential element in humans and is much less toxic than the hexavalent one, which is recognised as a carcinogenic and mutagenic agent [2].

The wastewater from the dyes, pigments, metal cleaning, plating, leather and mining industries contain undesirable amount of chromium(VI) ions and therefore priority is given to regulate these pollutants at the discharge level. The maximum contaminant level goal of chromium for the drinking water is 0.05 mg/l as per the World Health Organization (WHO) set standard [3]. Depuration technologies usually adopted to remove chromium from industrial wastewaters include precipitation, membrane filtration, solvent extraction with amines, ion exchange, activated carbon adsorption, electro-deposition, and various biological processes [4–9]. The choice of treatment depends on effluent characteristics such as concentration of chromium(VI), pH, temperature, flow volume, biological oxygen demand (BOD), the economics involved and the social factor like standard set by government agencies.

Adsorption is a versatile treatment technique practiced widely in fine chemical and process industries for wastewater and waste gas treatment. The usefulness of the adsorption process lies in the operational simplicity and reuse potential of adsorbents during long-term applications. Activated carbon adsorption has proved to be the least expensive treatment option, particularly in treating low concentrations of wastewater streams and in meeting stringent treatment levels. Activated carbon is a black solid substance resembling granular or powder charcoal and are carbonaceous material that have highly developed porosity, internal surface area and relatively high mechanical strength. Activated carbon-based systems can remove a wide variety of toxic pollutants with very high removal efficiencies. For these reasons, activated carbon adsorption has been widely used for the treatment of chromium containing wastewaters [10–12]. However, commercially available

* Corresponding author. Tel.: +91 3222 283958(O)/2283959(R); fax: +91 3222 282250.
E-mail address: bcmeikap@che.iitkgp.ernet.in (B.C. Meikap).

1385-8947/$ – see front matter © 2008 Elsevier B.V. All rights reserved.
doi:10.1016/j.cej.2008.11.035

Nomenclature

$1/n$	adsorption intensity (dimensionless)
b	Langmuir constant (l/g)
C_e	equilibrium lead(II) concentration (mg/l)
C_o	initial lead(II) concentration (mg/l)
D_i	effective diffusion coefficient (m^2/s)
d_p	diameter of the adsorbent particles (mm)
F	represents the fraction of solute adsorbed at any time t (mg/g)
k	measure of adsorbent capacity (l/g)
K	the constant obtained by multiplying K_L and b (Langmuir's constants) (mg l/g^2)
K_2	equilibrium rate constant of pseudo-second-order adsorption (min^{-1})
K_{ad}	equilibrium rate constant of pseudo-first-order adsorption (min^{-1})
K_c	equilibrium constant (dimensionless)
k_{id}	rate constants of intraparticle diffusion (mg/g $min^{-1/2}$)
K_L	Langmuir constant (mg/g)
M	mass of the adsorbent per unit volume (g/l)
q_e	amount of lead(II) adsorbed at equilibrium (mg/g)
R	radius of the adsorbent particles (μm)
S_s	outer specific surface of the adsorbent particles per unit volume of particle free slurry (g/m^3)
T	temperature (°C)
t	time (min)
V	volume of the solution (l)
W	weight of adsorbent (g)
β_1	mass transfer coefficient (cm s^{-1})
ΔG°	free energy of adsorption (kJ mol^{-1})
ΔH°	heat of adsorption (kJ mol^{-1})
ΔS°	standard entropy (k cal mol^{-1} K^{-1})

Greek letters

δ_p	density of the adsorbent particles (g/l)
ε_p	porosity of the adsorbent particles (m Dc)

activated carbons may be expensive and, for this reason, any cheap material, with a high carbon content and low inorganic, can be used as a raw material for the production of activated carbon. The materials developed for this purpose range from agricultural waste products, biomass and various solid substances. Some examples are activated groundnut husk carbon [13], coconut husk and palm pressed fibers [14], coconut shell [15], wood and dust coal activated carbons [16,17], coconut tree sawdust carbon [18], rice husk carbon [19], almond shell carbon [20], fly ash [21], agricultural wastes [22] have been reported in literature.

Most of the activated carbons are produced by a two-stage process carbonization followed by activation. The first step is to enrich the carbon content and to create an initial porosity and the activation process helps in enhancing the pore structure. Basically, the activation is two different processes for the preparation of activated carbon: physical activation and chemical activation. There are two important advantages of chemical activation in comparison to physical activation. One is the lower temperature in which the process is accomplished. The other is that the global yield of the chemical activation tends to be greater since burn off char is not required. Among the numerous dehydrating agents, zinc chloride in particular is the widely used chemical agent in the preparation of activated carbon [23]. Knowledge of different variables during the activation process is very important in developing the porosity of carbon sought for a given application. Chemical activation by zinc chloride improves the pore development in the carbon structure, and because of the effect of chemicals, the yields of carbon are usually high [24].

Table 1
Physico-chemical characteristics of the activated *Tamarind wood*.

Parameters	Values
Moisture (%)	10
Ash (%)	4.55
Volatile matter (%)	36.48
Fixed carbon (%)	48.97
Bulk density (g/ml)	0.791
BET surface area (m^2/g)	1322
Total pore volume (cm^2/g)	1.042
Mean pore radius (Å)	5.3

In this work it has been reported the results obtained on the preparation of activated carbon from *Tamarind wood* with zinc chloride activation and their ability to remove chromium(VI) from wastewater. The influence of several operating parameters for adsorption of chromium(VI), such as contact time, initial concentration, temperature, pH, particle size and adsorbent dose, etc. were investigated in batch mode. The kinetic data were fitted to different models and the isotherm equilibrium data were fitted to Langmuir and Freundlich.

2. Experimental technique

2.1. Adsorbate: chromium(VI)

A stock solution of chromium(VI) was prepared (1000 mg/l) by dissolving required amount of, potassium dichromate ($K_2Cr_2O_7$)

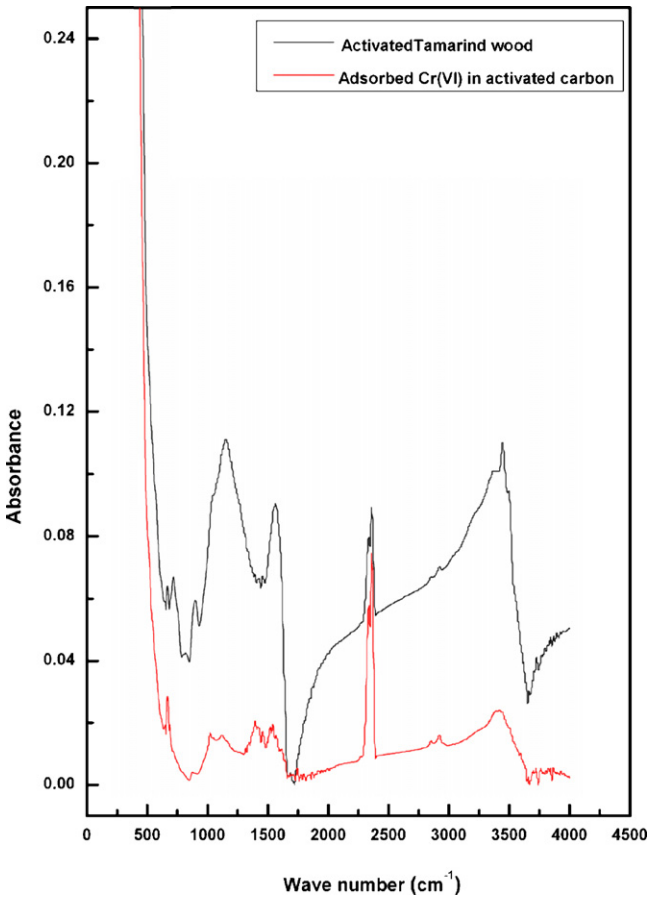

Fig. 1. FTIR result of prepared activated carbon and adsorbed with chromium(VI).

Table 2
Adsorption isotherms parameter at pH 6.5 and temperature = 30 °C for chromium(VI) removal.

Parameters	K_L (mg/g)	b (l/g)	R^2	K (1/g)	1/n
Values	28.019	0.0256	0.9951 Langumir 0.9967 Freundlich	1.8765	0.6555

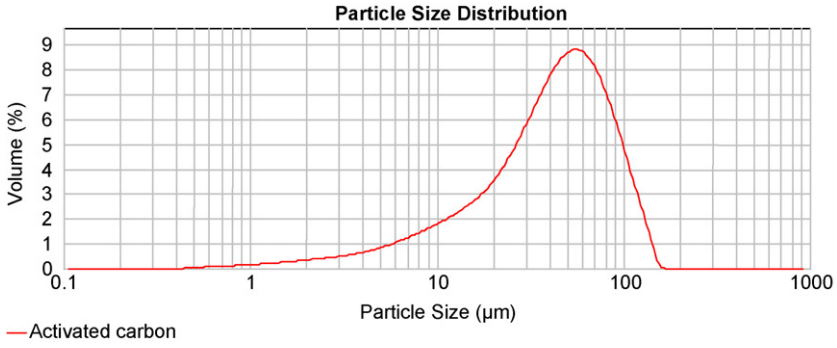

Fig. 2. Particle size distribution of ATW measured using Malvern Master Size.

in distilled water. The stock solution was diluted with distilled water to obtain desired concentration ranging from 10 to 50 mg/l. All the chemicals used in the study were from Merck (India) Ltd. and Qualigens Glaxo (India) Ltd. analytical grade.

2.2. Adsorbent: Tamarind wood activated

The *Tamarind wood* was collected from Indian Institute of Technology campus of Kharagpur, West Bengal, India and washed with deionized water four to five times for removing dirt and dust par-

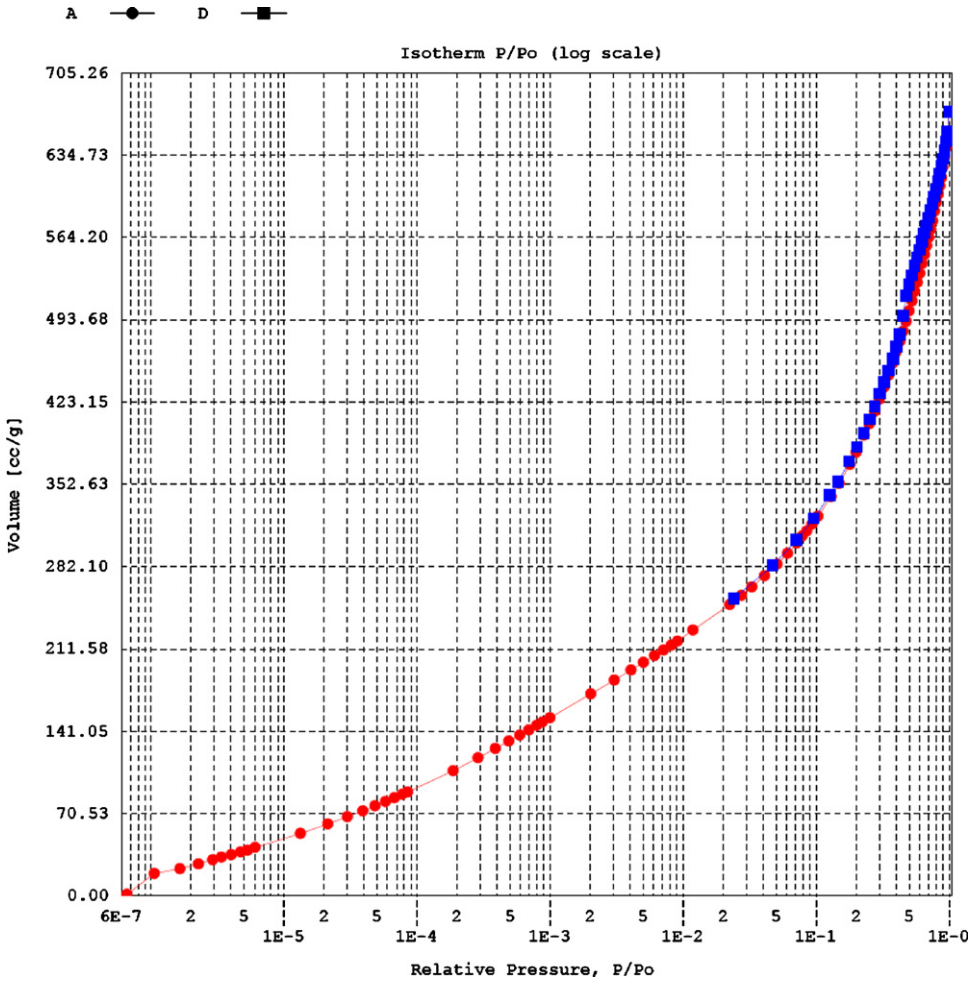

Fig. 3. N_2 adsorption/desorption isotherm of prepared activated carbon.

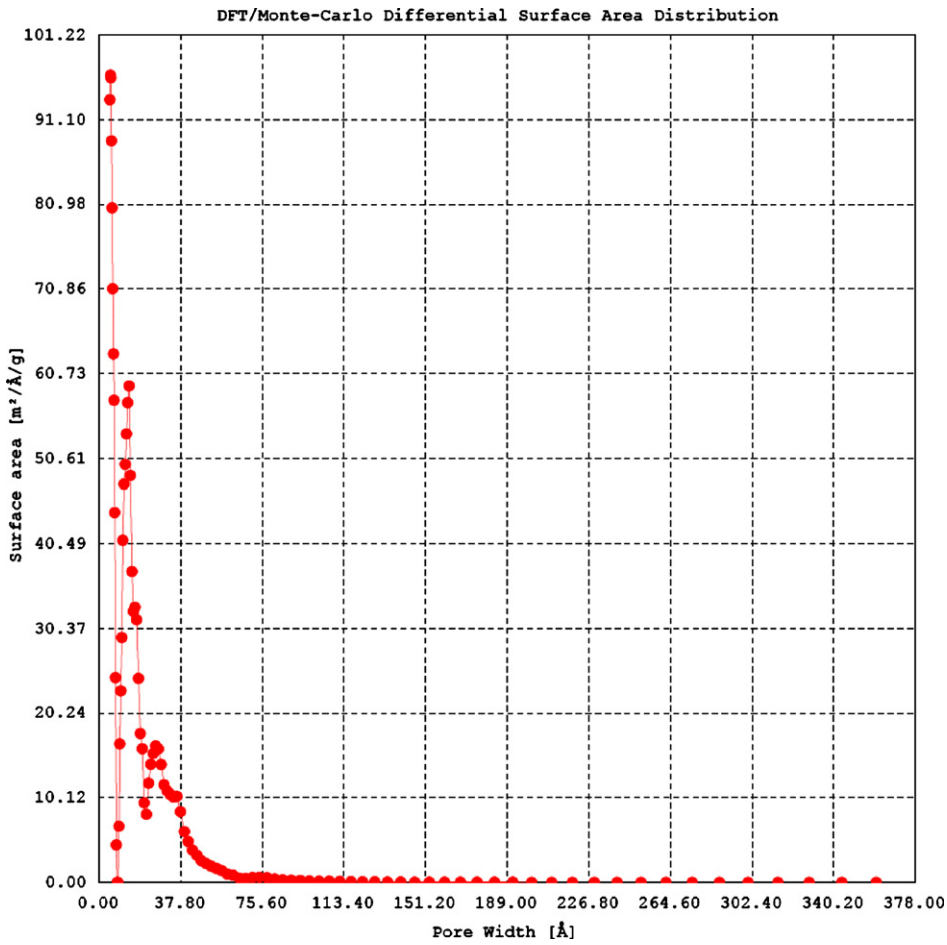

Fig. 4. Determination of pore size distribution of prepared activated carbon using DFT.

ticles. The washed wood was cut into 50.8–76.2 mm pieces. The woods were sun dried for 20 days. Chemical activation of the precursor was done with $ZnCl_2$. 10 g of dried precursor was well mixed with distilled water so that 100 ml concentrated solution contained 10 g of $ZnCl_2$. The chemical ratio is defined as the ratio of chemical activating agent ($ZnCl_2$) to the precursor. The chemical ratio (activating agent/precursor) was 100% in this case. The mixing was performed at 50 °C for 1 h. After mixing, the slurry was subjected to vacuum drying at 100 °C for 24 h. The resulting chemical-loaded samples were placed in a stainless-steel tubular reactor and heated (5 °C/min) to the final carbonization temperature under a nitrogen flow rate of 150 ml/min STP. Samples were held at the final temperature (carbonization temperature) for carbonization times of 40 min before cooling down under nitrogen. Nitrogen entering in the reactor was first pre-heated to 250–300 °C in a pre-heater. The products were washed sequentially with 0.5N HCl, hot water and finally cold distilled water to remove residual organic and mineral matters, and then dried at 110 °C. In all experiments, heating rate and nitrogen flow was kept constant. The experiments were carried out for chemical ratio (296%), activation time (40 min) and carbonization temperature (439 °C), this was the optimization condition find out using response surface methodology. Then carbon was dried to 60 °C. After this, carbon was crushed in a small ball mill with 50 numbers of small balls for 1 h. The powder from ball mill was collected and dried to remove the moisture. Then this powder carbon was kept in air-tight packet for the experimental use. The various physico-chemical characteristics of the prepared activated carbon were given in Table 1.

Atomic-absorption spectrophotometry utilizes the phenomenon that atoms absorb radiation of particular wavelength. By atomic-absorption spectrophotometer, the metals in water sample can be analyzed. It consists of four basic structural elements; a light source (hollow cathode lamp), an atomizer section for atomizing the sample (burner for flame, graphite furnace for electro thermal atomization), a monochrometer for selecting the analysis wavelength of the target element, and a detector for converting the light into an electrical signal. It detect concentration of chromium(VI) in parts per million (ppm) level in the solution and volume of sample required is only 1 ml for one analysis.

2.3. Method of experiment

Batch adsorption experiments were performed by contacting 0.2 g of the selected activated samples with 100 ml of the aqueous solution of different initial concentration (10, 20, 30, 50 mg/l) at natural solution pH (5.68). The experiments were performed in a thermal shaker at controlled temperature (30 ± 2 °C) for a period of 1 h at 120 rpm using 250 ml Erlenmeyer flasks containing 100 ml of different chromium(VI) concentrations at room temperature. Continuous mixing was provided during the experimental period with a constant agitation speed of 120 rpm for better mass transfer with high interfacial area of contact. The remaining concentration of chromium(VI) in each sample after adsorption at different time

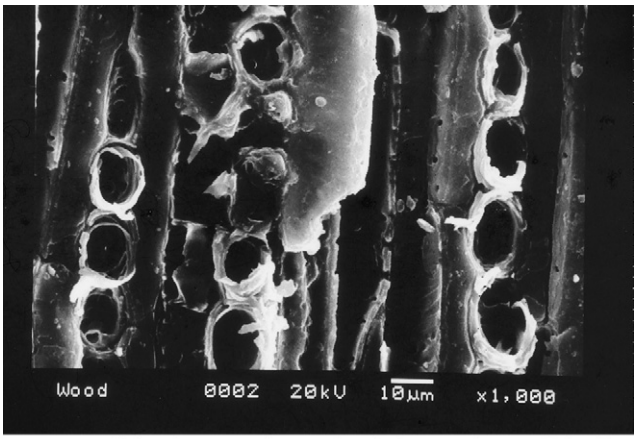

(a). Scanning electron micrograph (1000×) of precursor (raw *Tamarind wood*).

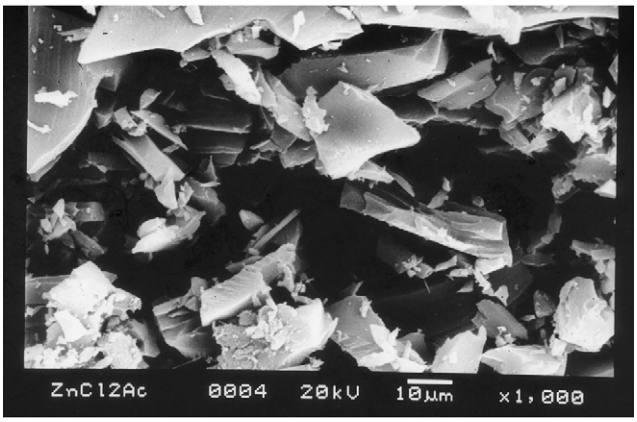

(b). Scanning electron micrograph (1000×) of prepared activated carbon.

Fig. 5. (a) Scanning electron micrograph (1000×) of precursor (raw *Tamarind wood*). (b) Scanning electron micrograph (1000×) of prepared activated carbon.

intervals was determined by atomic-absorption spectroscopy after filtering the adsorbent with Whatmen filter paper to make it carbon free. The batch process was used so that there is no need for volume correction. The chromium(VI) concentration retained in the adsorbent phase was calculated according to

$$q_e = \frac{(C_i - C_e)V}{W} \quad (1)$$

where C_i and C_e are the initial and equilibrium concentrations (mg/l) of chromium(VI) solution, respectively; V is the volume (l); and W is the weight (g) of the adsorbent. Two replicates per sample were done and the average results are presented.

The effect of adsorbent dosages (1–5 g/l) on the equilibrium adsorption of chromium(VI) on the selected carbon was investigated by employing different initial concentrations (10, 20, 30 and 50 mg/l) at different temperature (10–50 °C). For these experiments, the flasks were shaken, keeping the pH at natural (6.2) constant and agitation speed (120 rpm) for the minimum contact time required to attain equilibrium, as determined from the kinetic measurements detailed above.

2.4. Characterization of the prepared activated carbon

2.4.1. Pore structure characterization

The pore structure of the precursor and modified carbons were analyzed using N_2 adsorption, X-ray diffraction (XRD), and scanning electron microscopy (SEM). The BET surface area, total pore volume and density functional theory (DFT) pore size distribution were determined from nitrogen adsorption/desorption isotherms measured at −194 °C (boiling point of nitrogen gas at atmospheric pressure) by a Quantachrome Autosorb-I. Prior to gas adsorption measurements, the activated carbon was degassed at 200 °C in a vacuum condition for a period at least 4 h. The BET surface area was determined by means of the standard BET equation applied in the relative pressure range from 0.05 to 0.30. The total pore volume was calculated at a relative pressure of approximately 0.98 and at this relative pressure all pores were completely filled with nitrogen gas. The DFT pore size distribution of activated carbon sample was obtained based on nitrogen adsorption isotherms, using Autosorb software package with medium regularization.

Powder X-ray diffraction patterns were recorded on a Rigaku Miniflex Goniometer at 30 kV and 15 mA (Cu Kα radiation). Scanning electron microscopy analysis was carried out on the activated carbon prepared under optimum conditions, to study its surface texture and the development of porosity. In this study, SEM images were recorded using JEOL JSM-6300F field emission SEM. A thin layer of platinum was sputter-coated on the samples for charge dissipation during SEM imaging. The sputter-coated was operated in an argon atmosphere using a current of 6 mA. The coated samples were then transferred to the SEM specimen chamber and observed at an accelerating voltage of 10 kV, 8 spot size, 4 aperture and 5 mm working distance.

2.4.2. Surface chemistry determination

The surface chemistry of the precursor and modified carbons were determined using Fourier transform infrared radiation (FTIR).

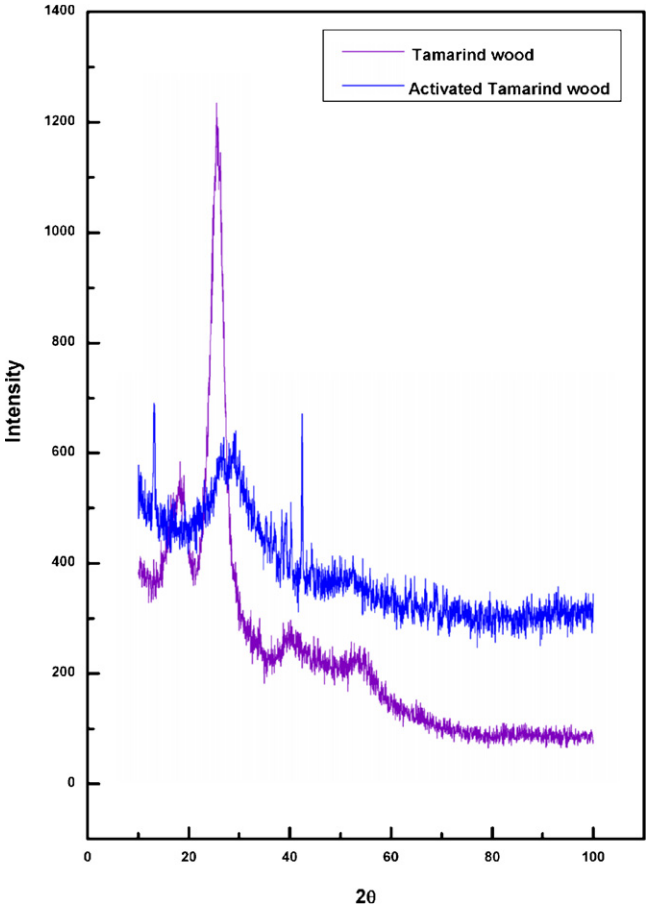

Fig. 6. X-ray diffraction result of precursor (raw *Tamarind wood*) and prepared activated carbon.

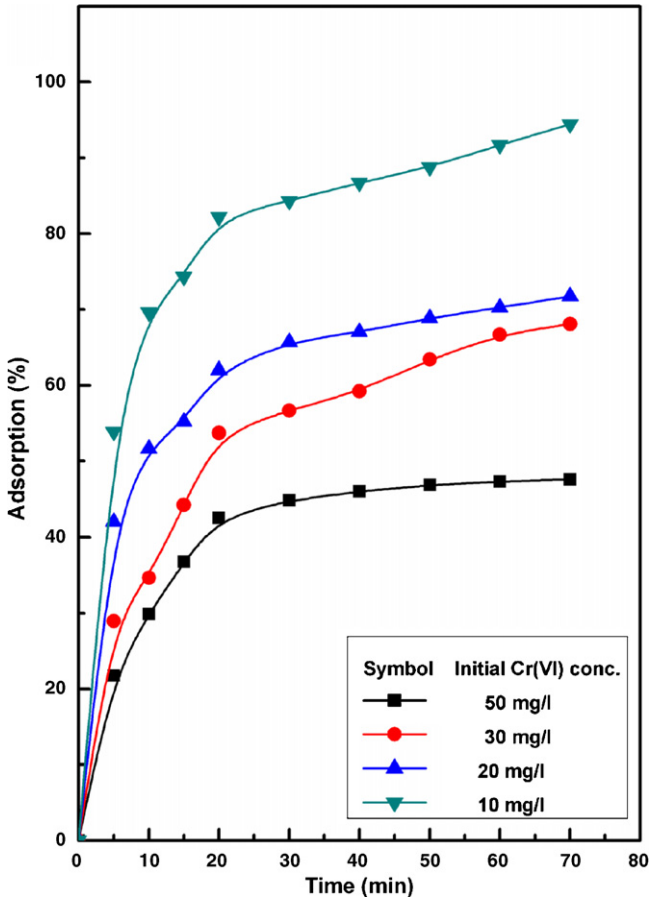

Fig. 7. Effect of contact time on adsorption of chromium(VI) at different initial feed concentration and at constant temperature 30 °C, adsorbent dose 2 g/l and pH 6.5.

FTIR analysis was applied on the same activated carbon to determine the surface functional groups, by using FTIR spectroscope (FTIR-2000, PerkinElmer), where the spectra were recorded from 400 to 4000 cm^{-1}.

2.4.3. Particle size analysis

Particle size analysis of powder activated carbon samples was done on using a Malvern instruments, mastersizer 2000 (UK). Samples were dispersed in water with the help of an ultrasonic magnetic stirrer before feeding into the instrument. Through use of laser diffraction technology, the technique of laser diffraction is based around principle that particles passing through a laser beam will scatter light at an angle that is directly related to their size. As the particle size decreases, the observed scattering angle increases logarithmically.

3. Results and discussions

3.1. Physical and chemical characterization of the adsorbent

3.1.1. Chemical properties

Adsorbent pH may influence the removal efficiency. Distinctly acidic adsorbent may react with the material to be removed and may hamper the surface properties of the adsorbent. The pH of activated *Tamarind wood* (ATW) was measured by using the method by Al-Ghouti et al. [25] as follows: 3 g of activated carbon was mixed with 30 ml of distilled water and agitated for 24 h. Then the pH value of the mixture was recorded with a pH meter. For our experiment the pH of ATW was found 6.77.

Ash content of the activated carbon is the residue that remains when the carbonaceous portion is burned off. The ash consists mainly of minerals such as silica, aluminum, iron, magnesium and calcium. Ash in activated carbon is not required and considered to be an impurity. Table 2 shows the proximity analysis of ATW. As the ash content is 4.55% it resembles good adsorbent.

The spectra of the prepared activated carbon, under the optimum preparation conditions and adsorbed chromium(VI) activated carbon were measured by an FTIR spectrometer within the range of 400–4000 cm^{-1} wave number. The FTIR spectrum plot obtained for the prepared activated carbon and adsorbed chromium(VI) activated carbon was shown in Fig. 1.

3.1.2. Physical properties

The smaller the particle sizes of a porous carbon, the greater the rate of diffusion and adsorption. Intraparticle diffusion is reduced as the particle size reduces, because of the shorter mass transfer zone, causing a faster rate of adsorption. Since we have prepared our carbon in a powdered form so it has a great efficiency of removal. The particle size analysis of the prepared activated carbon was done using Malvern analyzer. From Fig. 2 it shows that there are no particles above the size of 150 μm.

Density is particularly important in removal. If two carbons differing in bulk density are used at the same weight per liter, the carbon having higher bulk density will be able to remove more

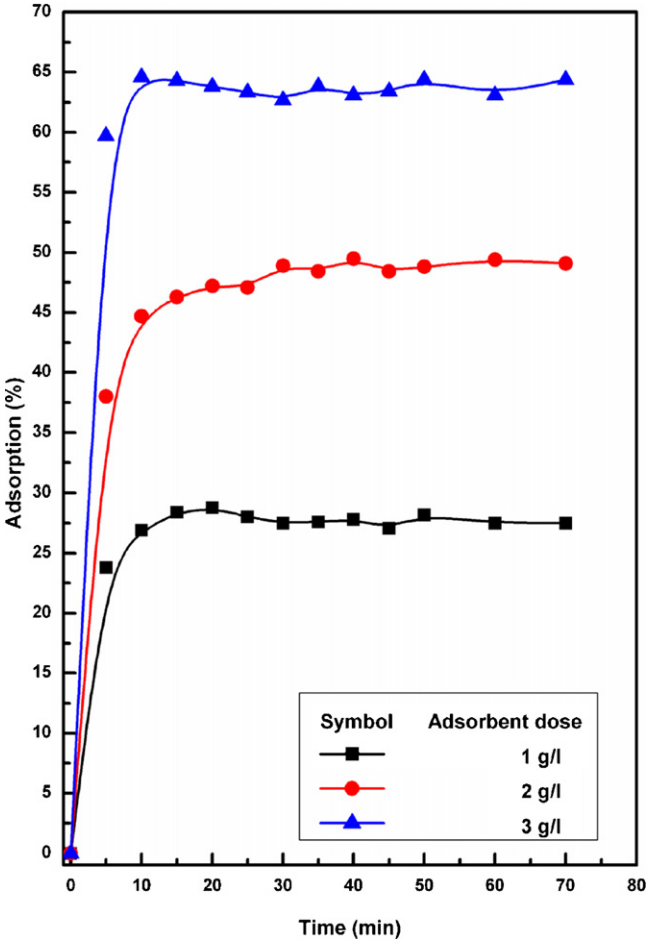

Fig. 8. Effect of contact time on adsorption of chromium(VI) at different adsorbent doses and at constant temperature 30 °C, initial feed concentration 50 mg/l and pH 6.5.

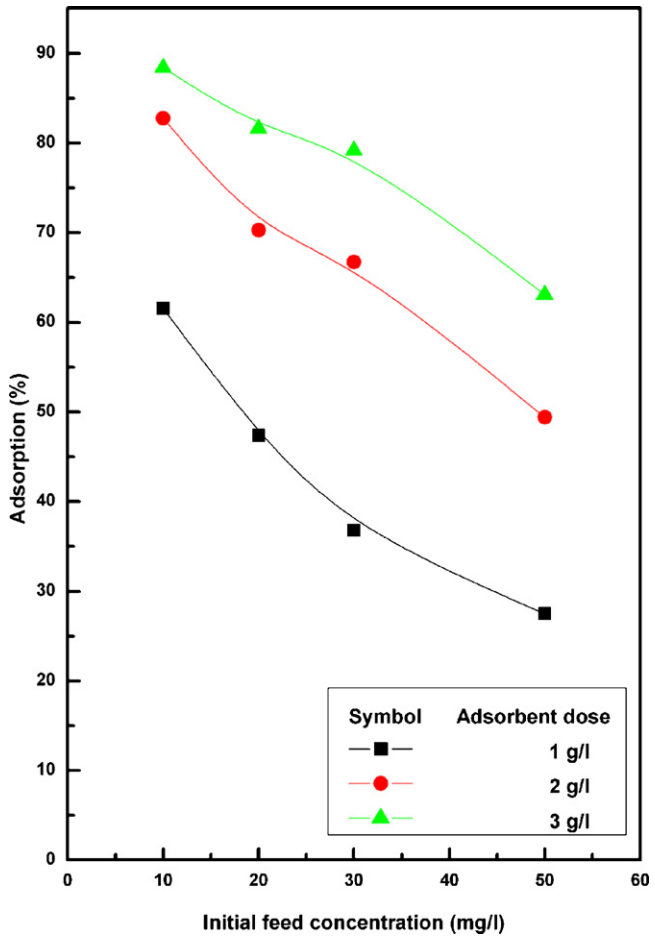

Fig. 9. Effect of initial feed concentration on adsorption of chromium(VI) at different adsorbent doses and at constant temperature 30 °C and pH 6.5.

efficiently. Average bulk density can be calculated by water displacement method. In this method, volume of water displaced is observed by a particular amount of carbon. The average bulk density was found to be 0.791 g/ml.

The BET surface area of ATW was measured from Fig. 3 and it was found 1322 m^2/g. The average pore diameter was found as 5.3 Å. This shows that ATW is reasonably good for adsorption. The DFT result is given in Fig. 4 and it shows that the activated carbon consists mainly pore width from 5 to 60 Å.

Fig. 5(a) and (b), respectively shows the scanning electron microscope images of the precursor (raw *Tamarind wood*) and the activated carbon obtained under the optimum preparation conditions. As can be seen from Fig. 5(a), there was very little pores available on the surface of the precursor. However, after $ZnCl_2$ treatment under the optimum preparation conditions, many large pores in a honeycomb shape were developed on the surface of the activated carbon and a smooth melt surface appeared, interspersed with generally large pores due to some of the volatiles being evolved as shown in Fig. 5(b).

The XRD result in Fig. 6 shows the crystalline structure of the carbon layers for the precursor (raw *Tamarind wood*) and prepared activated carbons. In general, there were no significant changes in the shape of the XRD graph for the precursor and prepared activated carbons. This confirms that the crystalline structure of the carbons remain unchanged after different thermal treatments. This result is expected since the treatments are limited only to moderate temperatures up to 439 °C. From the pore structure characterization, it can be seen that the thermal treatment used in this study caused insignificant effect on the textural properties of the carbons, thus confirms that the carbon pore structure was not altered by the thermal modification applied on the precursor.

3.2. Chromium adsorption

3.2.1. Contact time study

The relationship between contact time and chromium adsorption onto ATW at different initial chromium concentrations is shown in Fig. 7. The adsorption was very fast from the beginning to 20 min and the adsorption capacities increased from 39 to 95% with the chromium concentration range of 50–10 mg/l at a contact time of 20 min. With further increase of time, the adsorption kinetics decreased progressively, and finally the adsorption approached to equilibrium within 40 min in all the cases. The adsorption capacities corresponding to equilibrium adsorption increased from 44 to 99% with the decrease in chromium concentration from 50 to 10 mg/l. The fast adsorption at the initial stage is probably due to the increased concentration gradient between the adsorbate in solution and adsorbate in adsorbent as there must be increased number of vacant sites available in the beginning. The progressive increase in adsorption and consequently the attainment of equilibrium adsorption may be due to limited mass transfer of the adsorbate molecules from the bulk liquid to the external surface of ATW, initially and subsequently by slower internal mass transfer within the ATW particles.

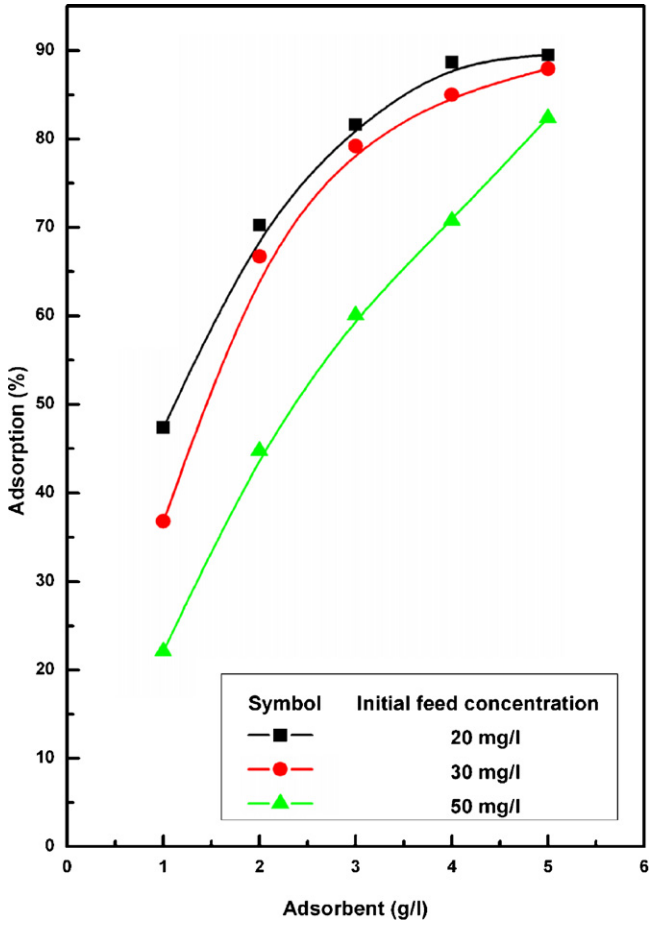

Fig. 10. Effect of adsorbent doses on adsorption of chromium(VI) at different initial feed concentration and at constant temperature 30 °C and pH 6.5.

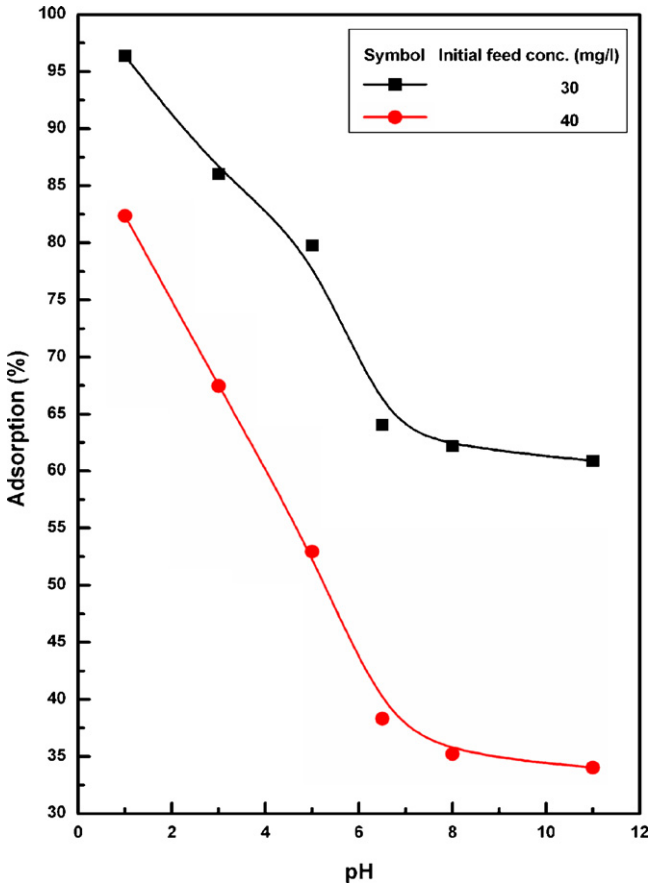

Fig. 11. Effect of pH on adsorption of chromium(VI) at different initial feed concentration at constant temperature 30 °C and adsorbent dose 2 g/l.

A comparison at different activated carbon dose (1, 2 and 3 g/l) with a constant temperature 30 °C and pH 6.5 has been made and presented in Fig. 8 for the adsorption efficiency. It has been found that under identical conditions higher doses of activated carbon enhances the removal efficiency of chromium. This is quite obvious that at higher dose activated carbon adsorb more quantity of chromium(VI), which resulted in increased efficiency.

3.2.2. Initial feed concentration

The effect of chromium concentration in the solution on the adsorption has been shown in Fig. 9. It can be seen from the figure that with increased initial feed concentration of chromium(VI), there was decrease in percentage of adsorption of chromium. The adsorption capacities for chromium(VI) decreased from 61 to 27%, 82 to 49% and 88 to 63% at adsorbent doses 1, 2 and 3 g/l, respectively with the increase in the initial feed concentration from 10 to 50 mg/l at constant temperature 30 °C and pH 6.5.

3.2.3. Adsorbent dose study

The effect of adsorbent dosage on the percentage removal chromium(VI) has been shown in Fig. 10. It can be seen from the figure that initially the percentage removal increases very sharply with the increase in adsorbent dosage but beyond a certain value 0.25–0.3 g, the percentage removal reaches almost a constant value. This trend is expected because as the adsorbent dose increases the number adsorbent particles increases and thus more chromium(VI) is attached to their surfaces. The adsorption capacities for chromium(VI) increased from 47 to 89%, 36 to 87% and 22 to 82% at 20, 30 and 50 mg/l initial feed concentration, respectively with the increase in the adsorbent doses from 1 to 5 g/l at constant temperature 30 °C and pH 6.5. A maximum removal of 89.5% was observed at adsorbent dosage of 5 g/l at pH 6.5 for an initial chromium(VI) concentration of 20 mg/l. Therefore, the use of 2 g/l adsorbent dose is justified for economical purposes.

3.3. Effect of solution pH on chromium adsorption

Earlier studies have indicated that solution pH is an important parameter affecting adsorption of heavy metals. Chromium(VI) removal was studied as a function of pH for two different initial concentrations for a fixed adsorbent dose (2 g/l) and the results are shown in Fig. 11. It is clear from this figure that the percent adsorption of chromium(VI) decreases with increase in pH from pH 1.0 to 6.0 and after pH 6.5 (natural pH) no adsorption takes place at all. It is important that the maximum adsorption at all the concentrations takes place at pH 1.0.

This behaviour can be explained considering the nature of the adsorbent at different pH in metal adsorption. The cell wall of activated carbon contains a large number of surface functional groups. The pH dependence of metal adsorption can largely be related to the type and ionic state of these functional groups and also on the metal chemistry in solution. Adsorption of chromium(VI) below pH 3.0 suggests that the negatively charged species (chromate/dichromate in the sample solution) bind through electrostatic attraction to positively charged functional groups on the surface of activated carbon because at this pH more functional groups carrying positive charge would be exposed. But at above pH 3.0, it seems that activated

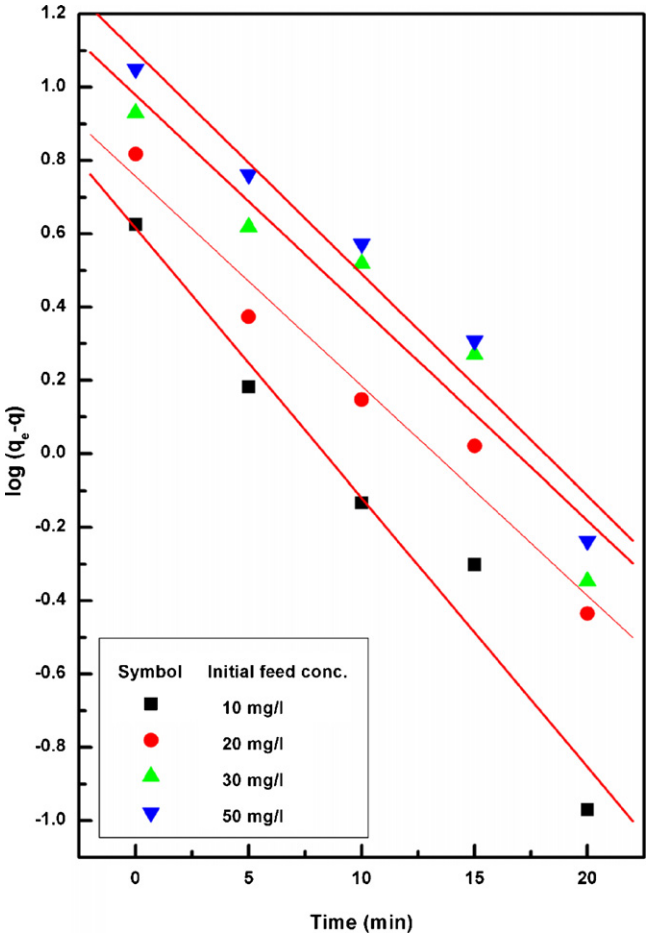

Fig. 12. Kinetics of chromium(VI) removal according to the Lagergren model at initial feed concentration of 10, 20, 30 and 50 mg/l.

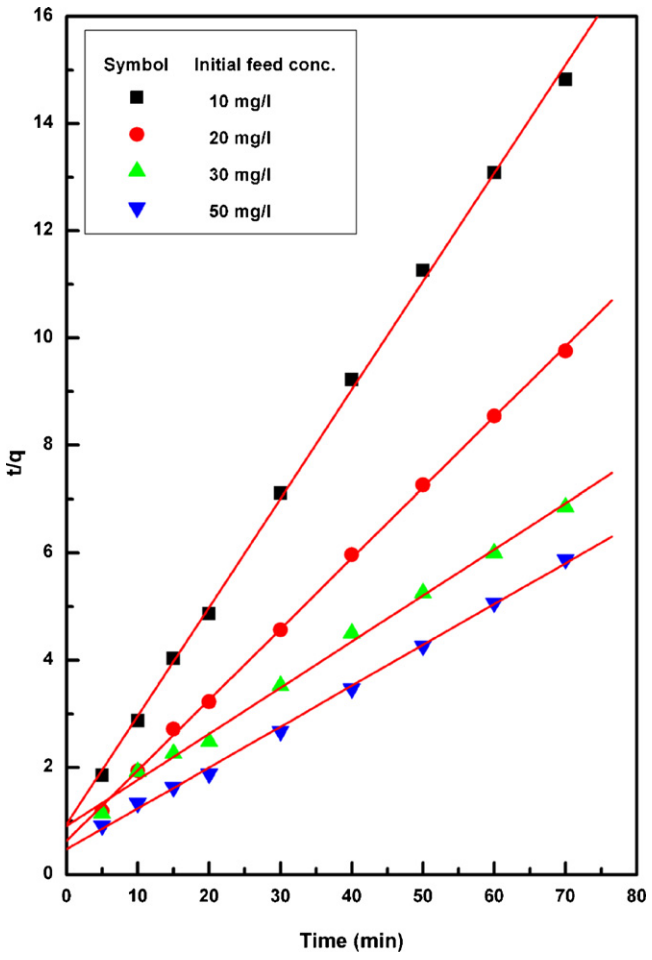

Fig. 13. Kinetics of chromium(VI) removal according to the pseudo-second-order model at initial feed concentration of 10, 20, 30 and 50 mg/l.

carbon possesses more functional groups carrying a net negative charge, which tends to repulse the anions. However, there is also the removal above pH 3.0, as indicated by Fig. 11, but the rate of removal is considerably reduced. Hence, it could be said that above pH 3.0, other mechanism like physical adsorption on the surface of adsorbent could have taken an important role in the adsorption of chromium(VI) and exchange mechanism might have reduced. In addition adjustment of pH is very important. The possibilities of other subsidiary substances and hydrogen bonding may affect the adsorption process and need careful analysis.

3.4. Adsorption kinetics models

In order to investigate the controlling mechanism of adsorption processes such as mass transfer and chemical reaction, the pseudo-first-order and pseudo-second-order equations are applied to model the kinetics of chromium adsorption onto ATW.

3.4.1. Pseudo-first-order model

Lagergren proposed a pseudo-first-order kinetic model. The integral form of the model is

$$\log(q_e - q) = \log q_e - \frac{K_{ad}}{2.303}t \quad (2)$$

where q is the amount of chromium(VI) sorbed (mg/g) at time t (min), q_e is the amount of chromium(VI) sorbed at equilibrium (mg/g), and K_{ad} is the equilibrium rate constant of pseudo-first-order adsorption (min^{-1}). This model was successfully applied to describe the kinetics of many adsorption systems.

3.4.2. Pseudo-second-order model

The adsorption kinetics may also be described by a pseudo-second-order reaction. The linearized-integral form of the model is

$$\frac{t}{q} = \frac{1}{K_2 q_e^2} + \frac{1}{q_e}t \quad (3)$$

where K_2 is the pseudo-second-order rate constant of adsorption.

The applicability of the above two models can be examined by each linear plot of $\log(q_e - q)$ versus t, and (t/q) versus t, respectively, and are presented in Figs. 12 and 13. To quantify the applicability of each model, the correlation coefficient, R^2, was calculated from these plots. The linearity of these plots indicates the applicability of the two models. However, the correlation coefficients, R^2, showed that the pseudo-second-order model, an indication of a chemisorptions mechanism, fits better the experimental data ($R^2 > 0.999$) than the pseudo-first-order model (R^2 is in the range of 0.958–0.981).

3.5. Effect of adsorbent particle size

The influence of particle size was studied for different initial feed concentration of chromium(VI) at constant temperature 30 °C and pH 6.5. Fig. 14 shows the experimental results obtained from a series of experiments performed using different particle sizes of ATW. The adsorption capacities for chromium(VI) increased from 67 to 91%, 39 to 64% and 30 to 49% at 10, 30 and 50 mg/l initial feed concentration, respectively with the decrease in the particle size from 52 to

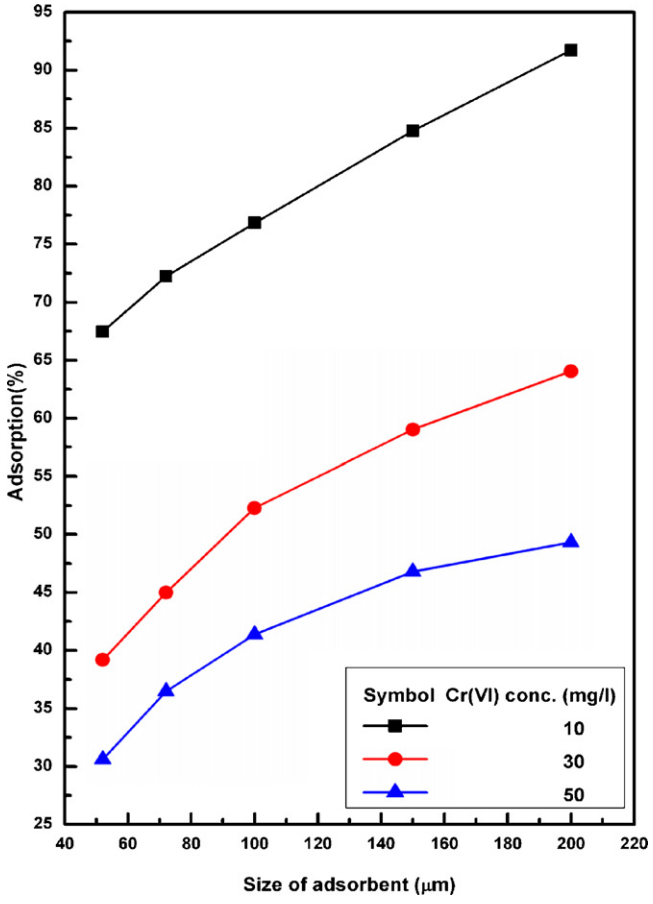

Fig. 14. Effect of size of adsorbent on adsorption of chromium(VI) at different initial feed concentration at constant temperature 30 °C, adsorbent dose 2 g/l and pH 6.5.

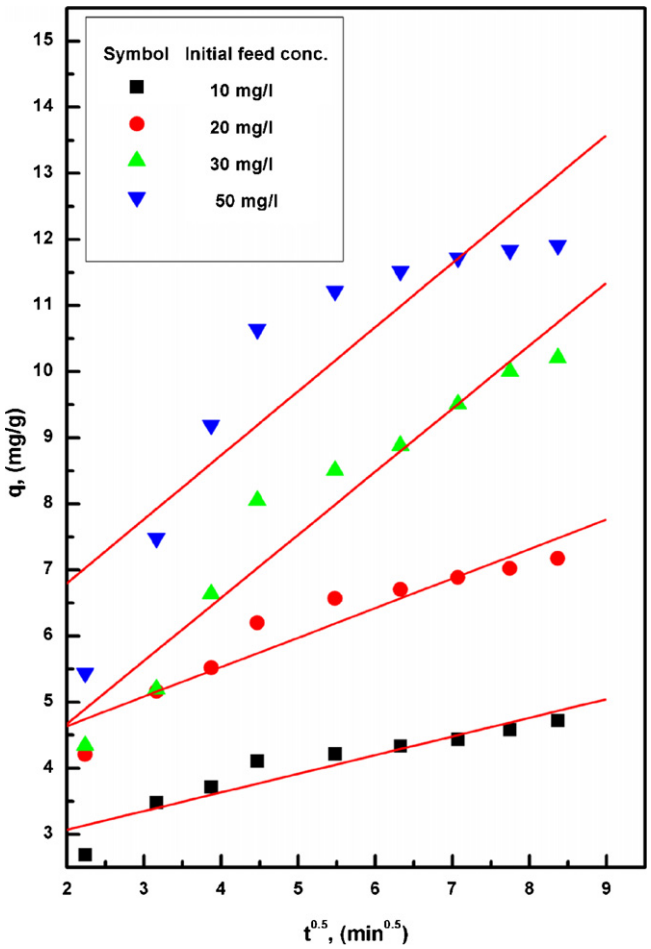

Fig. 15. Weber and Morris (intraparticle diffusion) plot for the adsorption of chromium(VI) for different initial feed concentration at pH 6.5, temperature 30 °C and adsorbent dosage 2 g/l.

200 μm because the higher adsorption with smaller adsorbent particle may be attributed to the fact that smaller particles give large surface areas. The result showed that there was a gradual increase of adsorption with the decrease in particle size.

3.6. Adsorption mechanisms

It is always important to predict the rate-limiting step in an adsorption process to understand the mechanism associated with the phenomena. For a solid liquid adsorption process, the solute transfer is usually characterized by either external mass transfer or intraparticle diffusion or both. Generally three types of mechanisms are involved in the adsorption process, mentioned as follows [26]:

1. Film diffusion, which involves the movement of adsorbate molecules from the bulk of the solution towards the external surface of the adsorbent.
2. Particle diffusion, where the adsorbate molecules move in the interior of the adsorbent particles.
3. Adsorption of the adsorbate molecules on the interior of the porous adsorbent.

3.6.1. Weber and Morris model

Intraparticle diffusion model is of major concern because it is rate-determining step in the liquid adsorption systems. During the batch mode of operation, there was a possibility of transport of sorbate species into the pores of sorbent, which is often the rate-controlling step. The rate constants of intraparticle diffusion (k_{id}) at different temperatures were determined using the following equation:

$$q = k_{id} t^{1/2} \tag{4}$$

where q is the amount sorbed at time t and $t^{1/2}$ is the square root of the time. The values of k_{id} (0.282, 0.446, 0.954 and 0.969 mg/g min$^{-1/2}$) at different initial feed concentrations 10, 20, 30, 50 mg/l, respectively, were calculated from the slopes of respective plot (q versus $t^{1/2}$ of Fig. 15) at later stages. Also from Fig. 16, it clears the dual nature for different temperatures 20, 30 and 40 °C at constant initial feed concentration 50 mg/l and pH 6.5. The dual nature of the curves was obtained due to the varying extent of adsorption in the initial and final stages of the experiment. This can be attributed to the fact that in the initial stages, adsorption was due to boundary layer diffusion effect whereas, in the later stages (linear portion of the curve) was due to the intraparticle diffusion effects. However, these plots indicated that the intraparticle diffusion was not the only rate controlling step because it did not pass through the origin.

3.6.2. Boyd model

Of the three steps, the third step is assumed to be very rapid and can be considered negligible. For design purposes, it is required to distinguish between film diffusion and particle diffusion. In order to identify the slowest step in the adsorption process, Boyd kinetic equation [27] was applied, which is represented as

$$F = 1 - \frac{6}{\pi^2} \exp(-Bt) \tag{5}$$

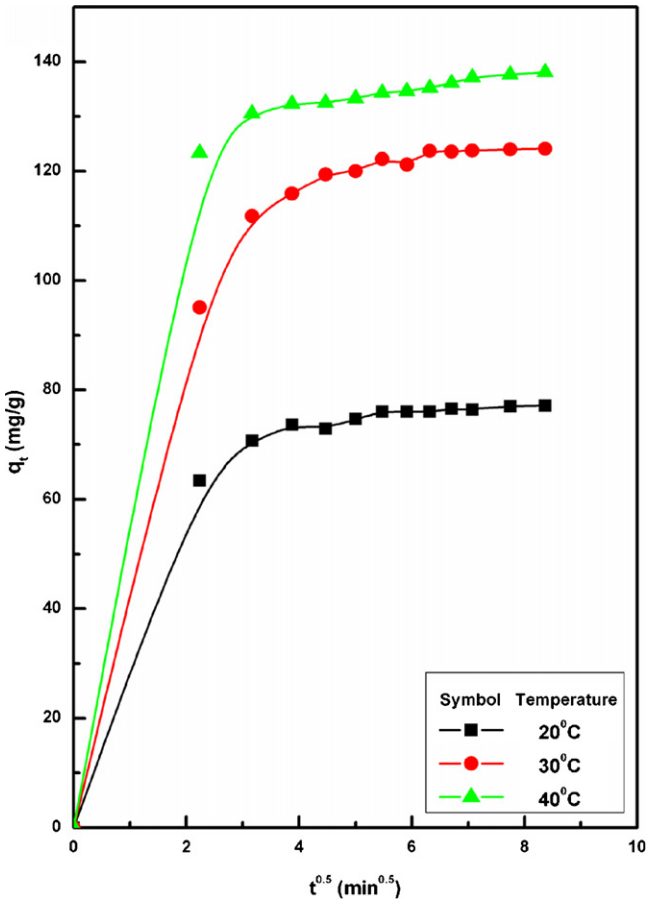

Fig. 16. Intraparticle diffusion plot at different temperatures for the initial concentration 50 mg/l, adsorbent dose 2 g/l and pH 6.5.

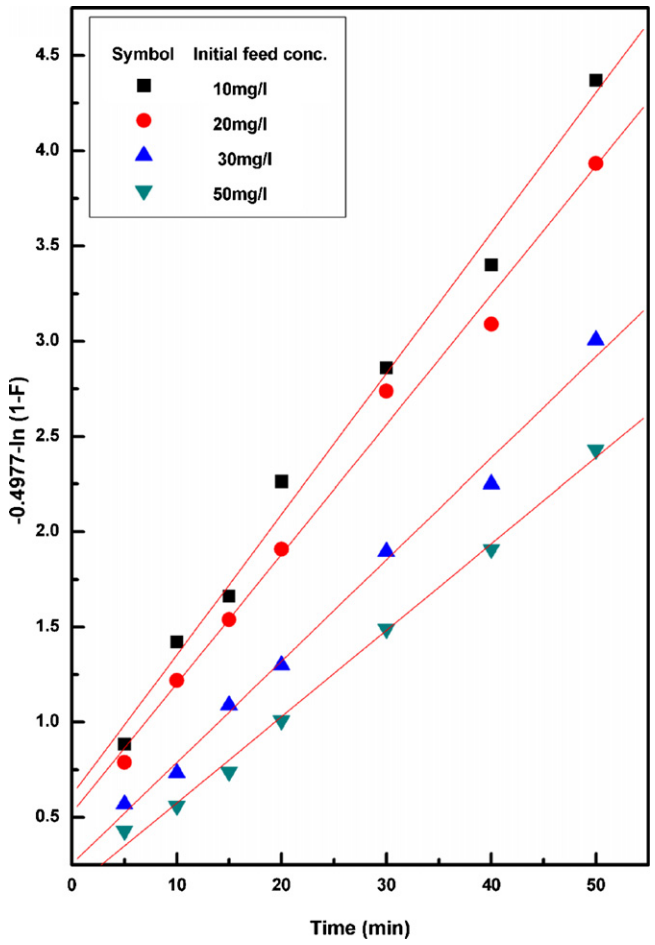

Fig. 17. Boyd plot for the adsorption of chromium(VI).

and

$$F = \frac{q}{q_e} \tag{6}$$

where q_e is the amount of chromium(VI) adsorbed at equilibrium (mg/g) and q represents the amount of chromium(VI) adsorbed at any time t (min), F represents the fraction of solute adsorbed at any time t, and Bt is a mathematical function of F. Eq. (5) can be rearranged by taking the natural logarithm to obtain the equation:

$$Bt = -0.4977 - \ln(1 - F). \tag{7}$$

The plot of $[-0.4977 - \ln(1 - F)]$ against time t can be employed to test the linearity of the experimental values. If the plots are linear and pass through origin, then the slowest (rate controlling) step in the adsorption process is the internal diffusion, and vice versa. From Fig. 17, it was observed that the plots are linear but do not pass though the origin suggesting that the adsorption process is controlled by film diffusion. The calculated B values were used to calculate the effective diffusion coefficient, D_i (m^2/s) using the relationship:

$$B = \frac{\pi^2 D_i}{r^2} \tag{8}$$

where D_i is the effective diffusion coefficient of solute in the adsorbent phase and r is the radius of the adsorbent particles. The D_i values were found to be 2.54×10^{-11}, 2.63×10^{-11}, 3.22×10^{-11} and 4.37×10^{-11} m^2/s, respectively for an initial chromium(VI) concentration of 10, 20, 30 and 50 mg/l.

3.6.3. McKay et al. model

During the present investigation, step (2) has been assumed rapid enough with respect to the other steps and therefore it is not rate limiting in any kinetic study. Taking in to account these probable steps, McKay et al. model [28] has been used for the present investigation:

$$\ln\left(\frac{C_e}{C_0} - \frac{1}{1+mK}\right) = \ln\left(\frac{mK}{1+mK}\right) - \left(\frac{1+mK}{mK}\right)\beta_1 S_s t \tag{9}$$

where m is the mass of the adsorbent per unit volume, K the constant obtained by multiplying K_L and b (Langmuir's constants), β_1 the mass transfer coefficient, and S_s is the outer specific surface of the adsorbent particles per unit volume of particle free slurry. The values of m and S_s were calculated using the following relations:

$$m = \frac{W}{V} \tag{10}$$

$$S_s = \frac{6m}{d_p \delta_p (1 - \varepsilon_p)} \tag{11}$$

where W is the weight of the adsorbent, V the volume of particle-free slurry solution, and d_p, δ_p and ε_p are the diameter, density and porosity of the adsorbent particles, respectively. The values of β_1 (4.467×10^{-4}, 7.419×10^{-4}, 9.903×10^{-4} and 1.192×10^{-3} $cm\,s^{-1}$) calculated from the slopes and intercepts of the plots (Fig. 18) of $\ln(C_e/C_0 - (1/1 + mK))$ versus t (min) at different initial feed concentration of chromium(VI) (10, 20, 30 and 50 mg/l). The values of β_1 obtained show that the rate of transfer of mass from bulk solution to the adsorbent surface was rapid enough so it cannot be rate-controlling step [29]. It can also be mentioned that the deviation

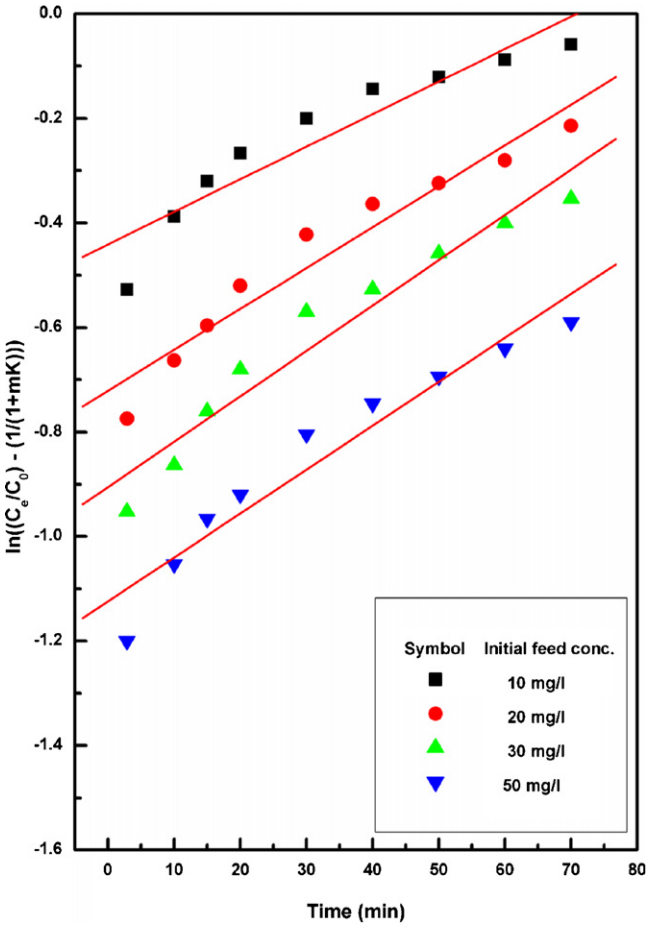

Fig. 18. Mass transfer plot for the adsorption of chromium(VI) at pH 6.5, initial concentration 50 mg/l, and adsorbent dosage 2 g/l.

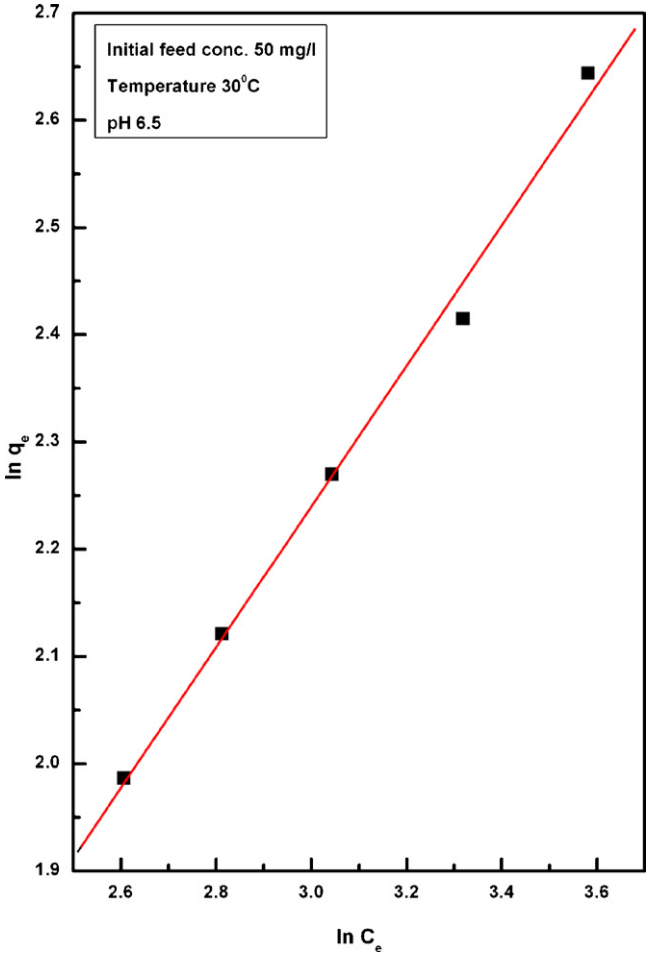

Fig. 19. Freundlich adsorption isotherm.

of some of the points from the linearity of the plots indicated the varying extent of mass transfer at the initial and final stages of the adsorption.

3.7. Adsorption isotherms

Several models have been used in the literature to describe the experimental data of adsorption isotherms. The Freundlich and Langmuir models are the most frequently employed models. In the present work both models were used.

The chromium(VI) adsorption isotherm followed the linearized Freundlich model as shown in Fig. 19. The relation between the metal uptake capacity 'q_e' (mg/g) of adsorbent and the residual metal ion concentration 'C_e' (mg/l) at equilibrium is given by

$$\ln\ q_e = \ln k + \frac{1}{n} \ln C_e \tag{12}$$

where the intercept $\ln k$ is a measure of adsorbent capacity, and the slope $1/n$ is the adsorption intensity. The isotherm data fit the Freundlich model well ($R^2 = 0.996$). The values of the constants k and $1/n$ were calculated to be 1.876 and 0.273, respectively. Since the value of $1/n$ is less than 1, it indicates a favorable adsorption.

The Langmuir equation relates solid phase adsorbate concentration (q_e), the uptake, to the equilibrium liquid concentration (C_e) as follows:

$$q_e = \left(\frac{K_L b C_e}{1 + bC_e}\right). \tag{13}$$

where K_L and b are the Langmuir constants, representing the maximum adsorption capacity for the solid phase loading and the energy constant related to the heat of adsorption, respectively. It can be seen from Fig. 20 that the isotherm data fits the Langmuir equation well ($R^2 = 0.995$). The values of K_L & b were determined from the figure and were found to be 28.019 mg/g and 0.025 l/mg, respectively. The outcome values of parameters k, n, K_L, b, R^2 for all the experiments with pH of solution equal to 6.5 for maximum removal of chromium(VI) are presented in Table 2.

3.8. Effect of temperature on chromium adsorption

Experiments were performed at different temperatures 20, 30 and 40 °C at a concentration of 50 mg/l and pH of 6.5. The adsorption increased from 27.5, 49.1 to 64.4% with the rise in temperature from 20 to 40 °C (Fig. 21). Equilibrium time for 20, 30 and 40 °C was found to be 30 min indicating that the equilibrium time was independent of temperature. Also Fig. 22 shows the effect of temperature for different initial feed concentration at constant adsorbent dose 2 g/l and pH 6.5. It can be seen from the figure that initially the percentage removal increases very sharply with the increase in temperature but beyond a certain value 30–40 °C, the percentage removal reaches almost a constant value. The above results also showed (Figs. 21 and 22) that, the adsorption was endothermic in nature. Since sorbent is porous in nature and possibilities of diffusion of sorbate cannot be ruled out therefore, increase in the adsorption with the rise of temperature may be diffusion controlled which is endothermic process, i.e. the rise of temperatures favors the sorbate transport with in the pores of sorbent [23]. The increased adsorption with the rise of temperature is also due to the

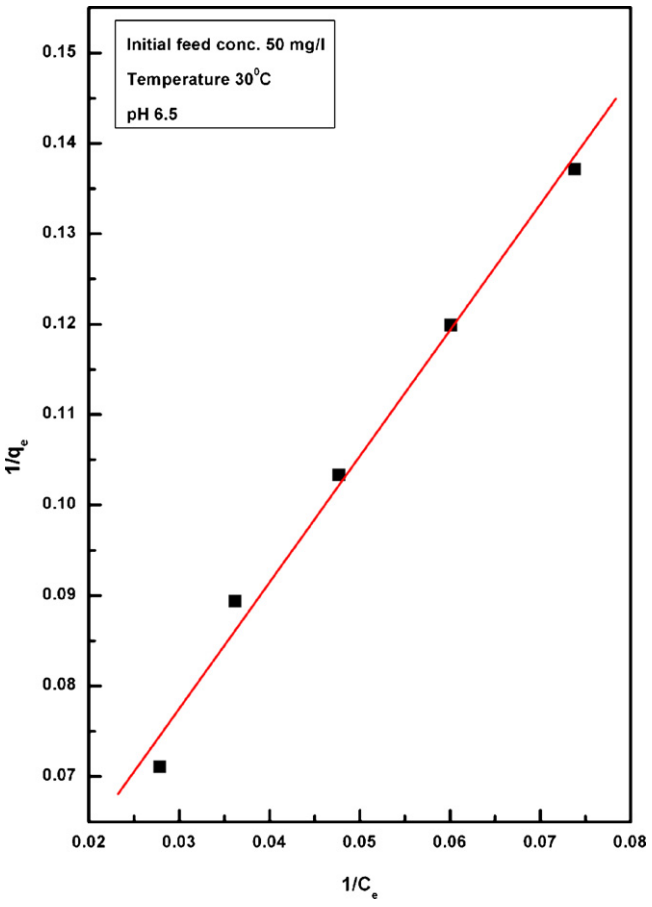

Fig. 20. Langmuir adsorption isotherm.

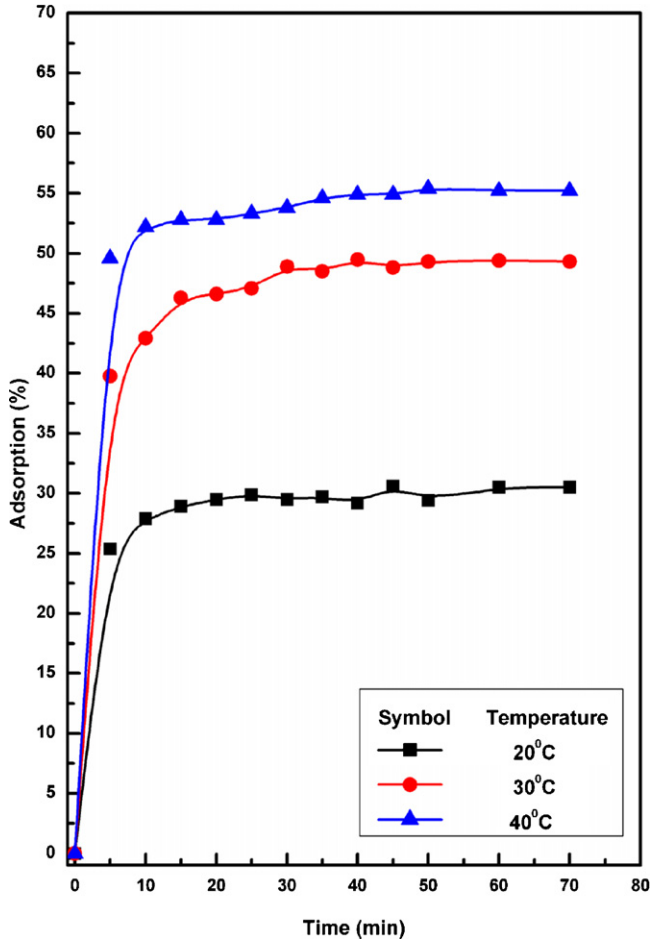

Fig. 21. Effect of temperature with time for the concentration of 50 mg/l at adsorbent dose 2 g/l and pH 6.5.

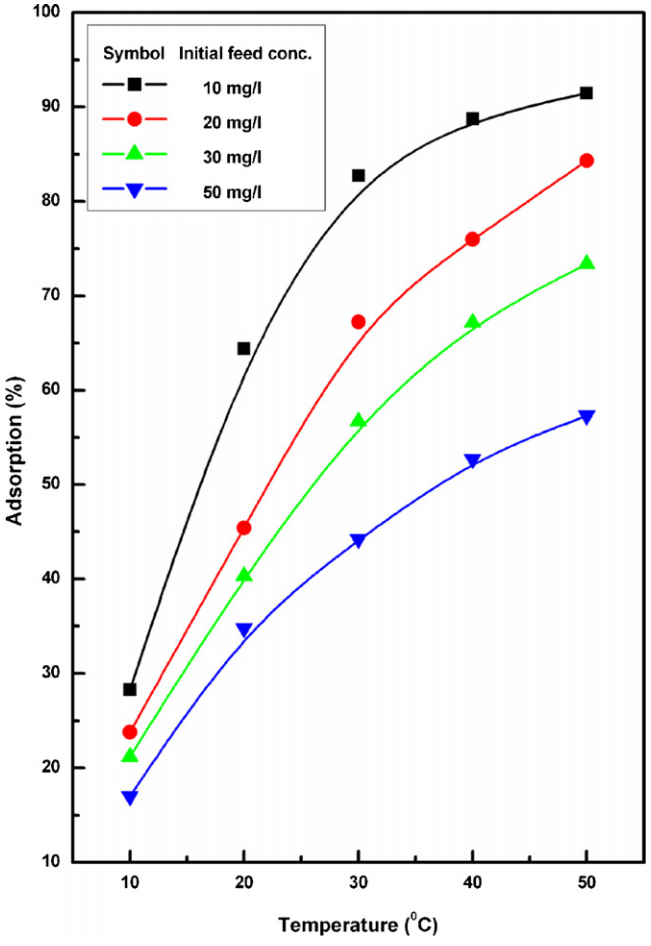

Fig. 22. Effect of temperature for different initial feed concentration at constant adsorbent dose 2 g/l and pH 6.5.

increase in the number of the adsorption sites generated because of breaking of some internal bonds near the edge of active surface sites of sorbent.

3.8.1. Thermodynamic parameters

Thermodynamic parameters such as free energy (ΔG°), enthalpy (ΔH°) and entropy (ΔS°) change of adsorption can be evaluated from the following equations [14,15]:

$$K_c = \frac{C_{Ae}}{C_e} \tag{14}$$

$$\Delta G_0 = -RT \ln K_c \tag{15}$$

where K_c is the equilibrium constant and C_{Ae} and C_e (both in mg/l) are the equilibrium concentrations for solute on the sorbent and in the solution, respectively. The K_c values are used in Eqs. (14) and (15) to determine the ΔG°, ΔH° and ΔS°. The K_c may be expressed in terms of the ΔH° (kJ mol^{-1}) and ΔS° (cal mol^{-1} K^{-1}) as a function of temperature:

$$\ln K_c = -\frac{\Delta H^\circ}{RT} + \frac{\Delta S^\circ}{R}. \tag{16}$$

Thermodynamic parameters such as free energy of adsorption (ΔG°), the heat of adsorption (ΔH°) and standard entropy (ΔS°) changes during the adsorption process were calculated using Eqs. (14)–(16) on a temperature range of 10–50 °C at different initial feed concentration of chromium(VI), (ΔH°) and (ΔS°) and were obtained from the slope and intercept of a plot of ln K_c against $1/T$ (Fig. 23). The values of these parameters are recorded in Table 3. The negative values of ΔG° indicate the spontaneous nature of the process and more negative value with increase of temperature shows that an increase in temperature favors the adsorption process. The positive values of ΔH° indicate that the adsorption process was endothermic in nature and the negative values of ΔS° suggest the probability of a favorable adsorption.

Table 3
Thermodynamic parameters for the adsorption of chromium(VI).

C_0 (mg/l)	ΔH° (kJ mol^{-1})	ΔS° (kJ mol^{-1} K^{-1})	ΔG° (kJ mol^{-1})				
			10 °C	20 °C	30 °C	40 °C	50 °C
10	53.529	0.1884	−107.16	−109.04	−110.93	−112.81	−114.69
20	53.695	0.1812	−104.99	−106.80	−108.61	−110.43	−112.24
30	44.158	0.1465	−85.63	−87.09	−88.56	−90.02	−91.49
50	34.544	0.1108	−65.91	−67.02	−68.13	−69.24	−70.35

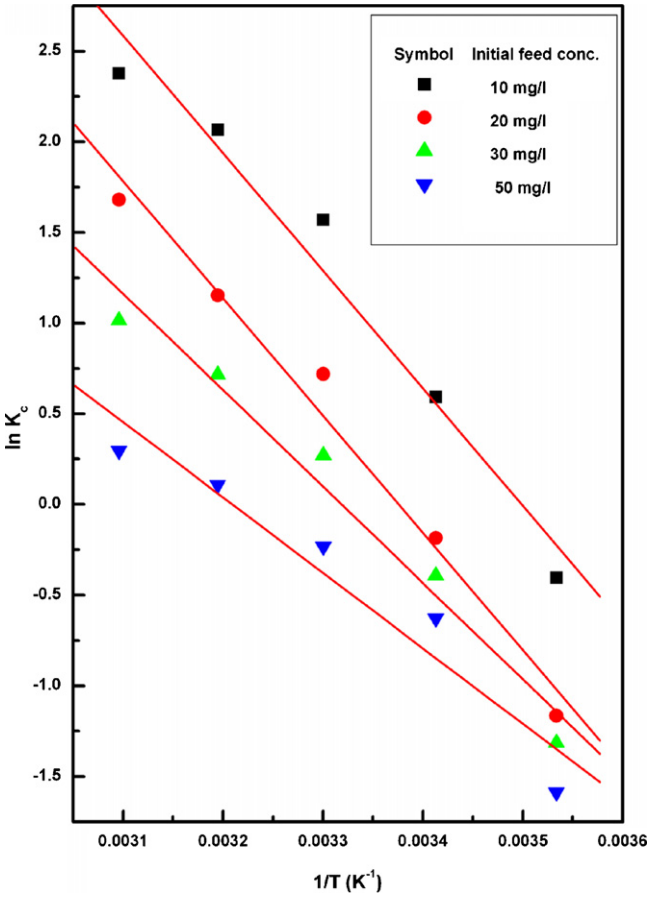

Fig. 23. A plot of ln K_c against $1/T$ for chromium(VI) adsorption for different initial feed concentration at constant adsorbent dose 2 g/l and pH 6.5.

4. Conclusions

Removal of chromium(VI) from aqueous solutions is possible using several abundantly available low-cost adsorbents. The present investigation shows that *Tamarind wood* activated carbon is an effective adsorbent for the removal of chromium(VI) from aqueous solutions. Conclusions from the present study are as follows:

- Characterization has shown a clear demarcation in the physico-chemical properties of the adsorbent.
- From the kinetics studies it is observed that adsorption of chromium(VI) is very rapid in the initial stage and decreases while approaching equilibrium. The equilibrium time increases with initial chromium(VI) concentration.
- The percentage removal of chromium(VI) increases with the increase in adsorbent dosage and decrease with increase in initial chromium(VI) concentration.
- Experimental results are in good agreement with Langmuir adsorption isotherm model, and have shown a better fitting to the experimental data. Adsorption of chromium(VI) obeys pseudo-second-order equation.
- The overall rate of chromium(VI) uptake was found to be controlled by pore diffusion, film diffusion and particle diffusion, throughout the entire adsorption period. Boyd plot confirmed that external mass transfer was the rate-limiting step in the adsorption process.
- Different thermodynamic parameters, viz., ΔH°, ΔS° and ΔG° have also been evaluated and it has been found that the adsorption was feasible, spontaneous and endothermic in nature. The positive value of the entropy change suggests the increased randomness.
- Under the prevailing conditions, the maximum chromium(VI) removal efficiency was found to be 99%. As the adsorbent is derived from an agricultural waste, activated carbon may be useful for the economic treatment of wastewater containing chromium(VI).

However, more investigations are needed on different types of industrial wastewaters and different operating conditions before such conclusions can be generalized.

References

[1] N. Serpone, E. Borgarello, E. Pelizzeti, E. Schiavello (Eds.), Photocatalysis and Environment, Kluwer Academic, The Netherlands, 1988.
[2] S.L. Brauer, K.E. Wetterhahn, Chromium(VI) forms a thiolate complex with glutathione, J. Am. Chem. Soc. 113 (8) (1991) 3001–3007.
[3] WHO, Guidelines for Drinking-Water Quality, 3rd ed., World Health Organization, Geneva, Switzerland, 2006, p. 54.
[4] D. Mohan, K.P. Singh, V.K. Singh, Removal of hexavalent chromium from aqueous solution using low-cost activated carbons derived from agricultural waste materials and activated carbon fabric cloth, Ind. Eng. Chem. Res. 44 (4) (2005) 1027–1042.
[5] G. Tiravanti, D. Petruzzelli, R. Passino, Pretreatment of tannery wastewaters by an ion exchange process for Cr(III) removal and recovery, Water Sci. Technol. 36 (2–3) (1997) 197–207.
[6] C.A. Kozlowski, W. Walkowiak, Removal of chromium(VI) from aqueous solutions by polymer inclusion membranes, Water Res. 36 (2002) 4870–4876.
[7] N. Kongsricharoern, C. Polprasert, Chromium removal by a bipolar electrochemical precipitation process, Water Sci. Technol. 34 (1996) 109–116.
[8] J.J. Testa, M.A. Grela, M.I. Litter, Heterogeneous photocatalytic reduction of chromium(III) over TiO_2 particles in the presence of oxalate: involvement of Chromium(VI) species, Environ. Sci. Technol. 38 (5) (2004) 1589–1594.
[9] V.K. Gupta, A.K. Shrivastava, N. Jain, Biosorption of chromium(VI) from aqueous solutions by green algae spirogyra species, Water Res. 35 (2001) 4079–4085.
[10] N.R. Bishnoi, M. Bajaj, N. Sharma, Adsorption of Chromium(VI) from aqueous and electroplating wastewater, Environ. Technol. 25 (8) (2004) 899–905.
[11] O.A. Fadali, Y.H. Magdy, A.A.M. Daifullah, E.E. Ebrahiem, M.M. Nassar, Removal of chromium from tannery effluents by adsorption, J. Environ. Sci. Health Part A: Toxic/Hazard. Subst. Environ. Eng. 39 (2) (2004) 465–472.
[12] V. Sarin, K.K. Pant, Removal of chromium from industrial waste by using eucalyptus bark, Bioresour. Technol. 97 (1) (2006) 15–20.
[13] K. Periasamy, K. Srinivasan, P.R. Murugananan, Studies on chromium(VI) removal by activated ground nut husk carbon, Indian J. Environ. Health 33 (1991) 433–439.
[14] W.T. Tan, S.T. Ooi, C.K. Lee, Removal of Chromium(VI) from solution by coconut husk and palm pressed fibres, Environ. Technol. 14 (1993) 277–282.
[15] C.P. Dwivedi, J.N. Sahu, C.R. Mohanty, B. Raj Mohan, B.C. Meikap, Column performance of granular activated carbon packed bed for Pb(II) removal, J. Hazard. Mater. 156 (1–3) (2008) 596–603.
[16] C.K. Singh, J.N. Sahu, K.K. Mahalik, C.R. Mohanty, B. Raj Mohan, B.C. Meikap, Studies on the removal of Pb(II) from wastewater by activated carbon developed from Tamarind wood activated with sulphuric acid, J. Hazard. Mater. 153 (2008) 221–228.
[17] C. Selomulya, V. Meeyoo, R. Amal, Mechanisms of Cr(VI) removal from water by various types of activated carbons, J. Chem. Technol. Biotechnol. 74 (1994) 111–122.
[18] K. Selvi, S. Pattabhi, K. Kadirvelu, Removal of Cr(VI) from aqueous solution by adsorption onto activated carbon, Bioresour. Technol. 80 (2001) 87–89.
[19] J.N. Sahu, S. Agarwal, B.C. Meikap, M.N. Biswas, Performance of a modified multi-stage bubble column reactor for lead(II) and biological oxygen demand removal from wastewater using activated rice husk, J. Hazard. Mater. 161 (1) (2009) 317–324.
[20] M. Kobya, Adsorption, kinetic and equilibrium studies of Cr(VI) by hazelnut shell activated carbon, Adsorpt. Sci. Technol. 22 (2004) 51–64.
[21] K. Rastogi, J.N. Sahu, B.C. Meikap, M.N. Biswas, Removal of methylene blue from wastewater using fly ash as an adsorbent by hydrocyclone, J. Hazard. Mater. 158 (2–3) (2008) 531–540.
[22] E. Demirbas, M. Kobya, E. Senturk, T. Ozkan, Adsorption kinetics for the removal of chromium(VI) from aqueous solutions on the activated carbons prepared from agricultural waster, Water SA 30 (2004) 533–539.
[23] K. Mohanty, M. Jha, B.C. Meikap, M.N. Biswas, Removal of chromium(VI) from dilute aqueous solutions by activated carbon developed from *Terminalia arjuna* nuts activated with zinc chloride, Chem. Eng. Sci. 60 (2005) 3049–3059.
[24] A. Ahmadpour, D.D. Do, The preparation of activated carbon from Macademia Nutshell by chemical activation, Carbon 35 (12) (1997) 1723–1732.
[25] M. Al-Ghouti, M.A.M. Khraisheh, S. Allen, M.N.M. Ahmad, The removal of dyes from textile wastewater: a study of the physical characteristics and adsorption mechanisms of diatomaceous earth, J. Environ. Manage. 69 (2003) 229–238.

[26] P. Chingombe, B. Saha, R.J. Wakeman, Sorption of atrazine on conventional and surface modified activated carbons, J. Colloid Interf. Sci. 302 (2006) 408–416.
[27] G.E. Boyd, A.W. Adamson, L.S. Myers Jr., The exchange adsorption of ions from aqueous solutions by organic zeolites, II: kinetics, J. Am. Chem. Soc. 69 (1947) 2836–2848.
[28] G. McKay, M.S. Otterburn, A.G. Sweeny, Surface mass transfer process during colour removal from effluents using silica, Water Res. 15 (1981) 321–331.
[29] G.S. Gupta, G. Prasad, V.N. Singh, Removal of colour from wastewater by sorption for water reuse, J. Environ. Sci. Health A 23 (1988) 205–218.